

Analytic Solution of Liquid Flow in Rectangular PDMS-GLASS Microchannel with Wall Slip and Electro-Viscous Effects^{*}

Wang Lei, Wu Jiankang⁽¹⁾ and Chen Bo

Mechanics Department, Huazhong University of Science & Technology
Wuhan National Laboratory for Optoelectronics, Wuhan 430074, China

Abstract. In microfluidic system flow slip velocity on solid wall can be the same order of magnitude as the characteristic velocity in microchannel. This paper presents an analytic solution of pressure-driven liquid flow velocity and flow-induced electric field in a rectangular microchannel made of polymer PDMS and GLASS with wall slip and electro-viscous effects. The Poisson-Boltzmann equation and the Navier-Stokes equation are solved for the analytic solutions. The analytic solutions well agree with the numerical solutions. The study results indicate that wall slip increases flow velocities in microchannel, the electro-viscous effect decreases flow velocities. The slip velocities on wide wall are larger than those on narrow wall. It is also found that the wall slip amplifies flow-induced electric field and enhances electro-viscous effect on flow.

Mathematics Subject Classification: 76W05

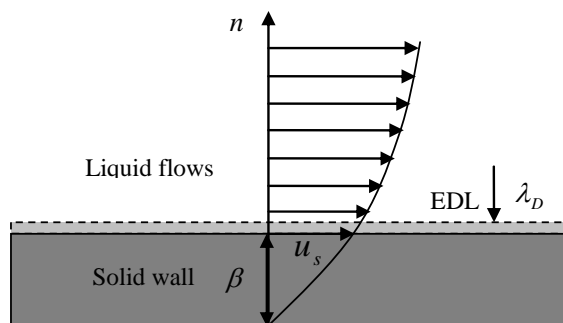
Keywords: Microchannel, Electric double layer, Wall slip, Electro-viscous effect

INTRODUCTION

In macroscopic flows the non-slip boundary condition on solid wall has been well accepted. A number of recent studies [2~11] have found evidences of slip velocities for liquid flow over hydrophobic surface (PDMS polymer materials). In general, the wall slip velocity is very small in comparison with average velocity in macroscopic channel. The wall slip velocity for liquid flow was first proposed by Navier in 1823, generally expressed as $u_s = \beta \partial u / \partial n$. The parameter β is called slip length ranging from several nanometers to several microns, and has been

-
- Project supported by Natural Science Foundation of China (Grant No.10872076)
 - (1) Wu Jiankang, Professor, Corresponding author, Email: wujkang@mail.hust.edu.cn

thought to be a property parameter of wall material and working fluid. The wall slip velocity is illustrated in following figure.



The wall slip length can be interpreted as an increase of channel width without slip velocity. The contribution of wall slip velocity to average velocity is the order of magnitude $O(\beta/h)$ [2], the ratio of slip length to flow scale (say channel width). The wall slip may play a significant role to flow-electricity interaction in microfluidic system. Finite difference method was used to solve flow velocities in rectangular microchannel with wall slip and electro-viscous effects [7]. The effect of wall slip on electrokinetic energy conversion in microfluidic system was examined [1], [13] based on the classical Onsager relation [12]. The wall slip was found to enhance electrokinetic energy conversion. In their studies the microchannel is two-dimensional and made of one kind of material. When in contacted with aqueous solution, most solid surfaces carry electrostatic charges that attract the counterions and repulse coions in the liquid. A thin charged liquid layer close to the solid wall is called electric double layer (EDL) [13]. When a pressure gradient is applied across a microchannel the charged fluid moves towards the downstream, results in a streaming current and induces an electric field. The flow-induced electric field, in return, applies an electric resistance on charged fluid in the direction opposite to flow, retards flow and decreases flow rate in microchannel. It is referred to as the electro-viscous effect [14 ~ 19]. The combinative effects of wall slip and electro-viscosity on flow in microfluidic system has not been well studied. Hydrophobic materials polydimethylsiloxane (PDMS) have become increasingly attractive for use in fabrication of microfluidic devices. However, PDMS is a soft polymer material, and easily deformed. It is an effective way to fix PDMS chips by bonding PDMS film on glass substrate. The flow behavior in PDMS channel is different from the glass channel due to different surface chemical properties. Glass is a hydrophilic material, does not show surface slip for aqueous solution in general. Furthermore, the wall zeta potential on PDMS surface is lower than that of glass surface when in contacted with electrolyte solution. The motivation of this work to seek an analytic solution of pressure-driven flows in rectangular PDMS/GLASS microchannel with wall slip and electro-viscous effects in order to gain a better understanding flow-electricity interaction in a complex microfluidic systems.

1. GOVERNING EQUATIONS AND BOUNDARY CONDITIONS

A rectangular microchannel is shown in Figure (1). The upper layer of the microchannel is made of PDMS which is bonded on a glass substrate.

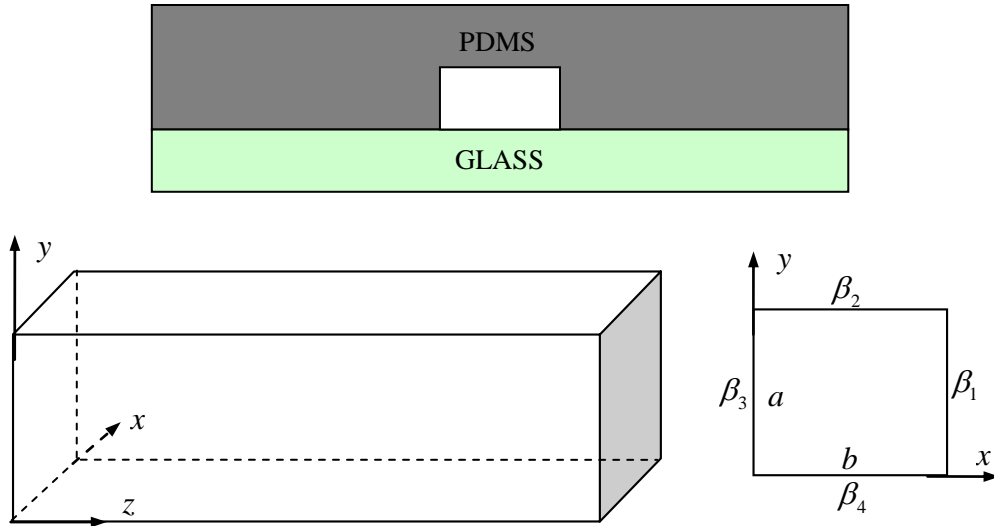


Fig.1 The sketch of rectangular microchannel

where a, b are the height and width of the channel section, respectively. When a pressure gradient is applied across the channel, flow in z direction is generated. Generally, body force except electric resistance can be ignored in microfluidic system. The continuity equation and Navier-Stokes equation of steady laminar flow for incompressible viscous fluid read as follows:

$$\frac{\partial w}{\partial z} = 0 \tag{1}$$

$$-\frac{dp}{dz} + \mu \nabla^2 w + \rho_e E_z = 0, \quad 0 \leq x \leq b, \quad 0 \leq y \leq a \tag{2}$$

Where ρ_e is volume charge density of fluid, E_z is flow-induced electric field. $\rho_e E_z$ is flow-induced electric resistance. The wall slip boundary conditions are specified as follows:

$$\begin{aligned} w = \beta_3 \frac{\partial w}{\partial x}, \quad x = 0, & \quad w = -\beta_1 \frac{\partial w}{\partial x}, \quad x = b \\ w = \beta_4 \frac{\partial w}{\partial y}, \quad y = 0, & \quad w = -\beta_2 \frac{\partial w}{\partial y}, \quad y = a \end{aligned} \tag{3}$$

Where $\beta_1, \beta_2, \beta_3, \beta_4$ are the slip lengths of the channel walls of different materials. For a symmetric electrolyte solution (1:1), the electric potential and volume charge density of electric double layer are governed by Poisson-Boltzmann equation (P-B) [1] :

$$\nabla^2 \varphi = \frac{2n_0 z e}{\varepsilon} \sinh\left(\frac{z e}{k_b T} \varphi\right) \quad (4)$$

$$\rho_e = -\varepsilon \nabla^2 \varphi \quad (5)$$

Where ε , z and n_0 are the dielectric constant, the ionic valence and the ionic number concentration of the bulk fluid, respectively. e is the charge of a proton, k_b is the Boltzmann constant, and T is the absolute temperature. The boundary conditions of equation (4) on wall are specified as follow:

$$\begin{aligned} \varphi = \zeta_3, \quad x = 0, \quad \varphi = \zeta_1, \quad x = b, \\ \varphi = \zeta_4, \quad y = 0, \quad \varphi = \zeta_2, \quad y = a, \end{aligned} \quad (6)$$

Where $\zeta_1, \zeta_2, \zeta_3, \zeta_4$ are the Zeta potentials of channel walls. Both wall slip velocity and electric double layer are tangent to channel wall. The wall slip velocity does not interfere electric double layer, thus the electric potential and charge density of electric double layer will not be modified by wall slip in an infinite uniform microchannel. The flow-induced electric field is related to flow velocity by electric current balancing condition [13] which states that the net current in microchannel must be zero in steady state, expressed as follows

$$I_s + I_c = 0 \quad (7)$$

Where I_s, I_c are the streaming current and the conductive current in microchannel, respectively.

$$I_s = \int_0^b \int_0^a w \rho_e \, dx dy \quad (8)$$

$$I_c = \lambda_b E_z ab \quad (9)$$

Where λ_b is the electric conductivity of bulk liquid. The flow-induced electric field is expressed as follows

$$E_z = -\frac{I_s}{\lambda_b ab} = -\frac{\int_0^b \int_0^a w \rho_e \, dx dy}{\lambda_b ab} \quad (10)$$

The equations (2), (4), (10) with boundary conditions (3), (6) are solved for flow velocity and flow-induced electric field in microchannel. For generality, the flow variables are normalized to dimensionless forms :

$$\bar{x} = \frac{x}{a}, \quad \bar{y} = \frac{y}{a}, \quad \bar{w} = \frac{w}{U}, \quad \bar{\beta} = \frac{\beta}{a}, \quad \bar{p} = \frac{p}{\rho U^2}, \quad \bar{Q} = \frac{Q}{\sigma a^2 U}, \quad (11)$$

$$\bar{\varphi} = \frac{\varphi}{\zeta_0}, \quad \bar{\rho}_e = \frac{\rho_e}{(-\varepsilon \zeta_0 / a^2)}, \quad \bar{E}_z = \frac{E_z}{[\varepsilon \zeta_0 U / (\sigma \lambda_b a^2)]}, \quad (12)$$

Where the characteristic velocity U is the maximum velocity in microchannel

without wall slip and electro-viscous effects, and U is proportional to pressure gradient, $\sigma = b/a$, the ratio of the width and the height of the channel section, ζ_0 is the characteristic surface electric potential, λ_b , μ are the electric conductivity and the dynamic viscosity of the bulk solution, wall electric conductivity is neglected in present study. Dimensionless P-B equation is expressed as

$$\nabla^2 \bar{\varphi} = \alpha_1 \sinh(\alpha_2 \bar{\varphi}), \quad \bar{\rho}_e = \nabla^2 \bar{\varphi} \tag{13}$$

Where $\alpha_2 = ze\zeta_0/(K_bT)$ is a dimensionless parameter reflecting properties of EDL, $\alpha_1 = (\kappa a)^2/\alpha_2$, κa is electrokinetic radius, the ratio of channel height to EDL thickness, $\kappa = 1/\lambda_D = [2n_0z^2e^2/(\epsilon K_bT)]^{1/2}$, λ_D is the EDL thickness. The boundary conditions of equation (13) are given as

$$\begin{aligned} \bar{\varphi} = \zeta_3/\zeta_0, \quad \bar{x} = 0, \quad \bar{\varphi} = \zeta_1/\zeta_0, \quad \bar{x} = \sigma, \\ \bar{\varphi} = \zeta_4/\zeta_0, \quad \bar{y} = 0, \quad \bar{\varphi} = \zeta_2/\zeta_0, \quad \bar{y} = 1, \end{aligned} \tag{14}$$

Equations (13), (14) can be numerically solved for charge density (see Appendix A). Dimensionless form of the flow equation (2) is written as follows

$$\nabla^2 \bar{w} = C + \gamma \bar{\rho}_e \bar{E}_z = F(\bar{x}, \bar{y}), \tag{15}$$

$$\text{Where } C = \frac{\rho U a}{\mu} \frac{\partial \bar{p}}{\partial z}, \quad \gamma = \frac{\epsilon^2 \zeta^2}{\sigma \mu \lambda_b a^2} \tag{16}$$

in which the parameter C is the ratio of pressure gradient to viscous force, and γ is defined as electro-viscous number reflecting the ratio of flow-induced electric resistance to viscous force. The dimensionless wall slip boundary conditions are written as

$$\bar{x} = 0, \quad \bar{w} = \bar{\beta}_3 \frac{\partial \bar{w}}{\partial \bar{x}}; \quad \bar{x} = \sigma, \quad \bar{w} = -\bar{\beta}_1 \frac{\partial \bar{w}}{\partial \bar{x}}, \tag{17}$$

$$\bar{y} = 0, \quad \bar{w} = \bar{\beta}_4 \frac{\partial \bar{w}}{\partial \bar{y}}; \quad \bar{y} = 1, \quad \bar{w} = -\bar{\beta}_2 \frac{\partial \bar{w}}{\partial \bar{y}}, \tag{18}$$

Dimensionless form of the electric field equation (10) is written as follows

$$\bar{E}_z = \int_0^\sigma \int_0^1 \bar{w} \bar{\rho}_e \, d\bar{x} d\bar{y} \tag{19}$$

2. ANALYTIC FLOW SOLUTION OF RECTANGULAR MICROCHANNEL WITH WALL SLIP AND ELECTRO-VISCOUS EFFECTS

Suppose general solution of flow equation (15) can be expanded as an infinite series of eigenfunctions.

$$\bar{w}(\bar{x}, \bar{y}) = \sum_{n=1}^{\infty} \sum_{m=1}^{\infty} w_{mn} \phi_{mn}(\bar{x}, \bar{y}), \quad (20)$$

where the eigenfunctions ϕ_{mn} are governed by following equation.

$$\frac{\partial^2 \phi_{mn}}{\partial \bar{x}^2} + \frac{\partial^2 \phi_{mn}}{\partial \bar{y}^2} = c_{mn} \phi_{mn}, \quad \text{and} \quad \phi_{mn}(\bar{x}, \bar{y}) = X_m(\bar{x}) \cdot Y_n(\bar{y}) \quad (21)$$

The general solutions of the eigenfunctions can be expressed as

$$\begin{aligned} X_m(\bar{x}) &= A_1 \sin(\lambda_m \bar{x}) + A_2 \cos(\lambda_m \bar{x}) \\ Y_n(\bar{y}) &= B_1 \sin(\kappa_n \bar{y}) + B_2 \cos(\kappa_n \bar{y}) \end{aligned} \quad (22)$$

Substituting equation (22) into equation (21) yields

$$c_{mn} = -(\lambda_m^2 + \kappa_n^2) \quad (23)$$

Making use of the boundary conditions (17), one may obtain

$$\begin{aligned} A_1 \sin(\lambda_m \sigma) + A_2 \cos(\lambda_m \sigma) &= -\bar{\beta}_1 \lambda_m (A_1 \cos(\lambda_m \sigma) - A_2 \sin(\lambda_m \sigma)) \\ A_2 &= \bar{\beta}_3 \lambda_m A_1 \end{aligned} \quad (24)$$

After rearrangement the equation (24) reduces to

$$ctg(\lambda_m \sigma) = \frac{\bar{\beta}_1 \bar{\beta}_3 \lambda_m^2 - 1}{(\bar{\beta}_1 + \bar{\beta}_3) \lambda_m} \quad (25)$$

Similarly, making use of the boundary conditions (18), yields

$$ctg(\kappa_n) = \frac{\bar{\beta}_2 \bar{\beta}_4 \kappa_n^2 - 1}{(\bar{\beta}_2 + \bar{\beta}_4) \kappa_n} \quad (26)$$

The eigenvalues λ_m, κ_n can be solved using Newton iterative algorithm (see Appendix B). So the eigenfunctions are expressed as follows

$$\phi_{mn} = [\sin(\lambda_m \bar{x}) + \bar{\beta}_3 \lambda_m \cos(\lambda_m \bar{x})] [\sin(\kappa_n \bar{y}) + \bar{\beta}_4 \kappa_n \cos(\kappa_n \bar{y})] \quad (27)$$

Expanding the forcing term of equation (15) as an infinite series of eigenfunctions ϕ_{mn}

$$F(\bar{x}, \bar{y}) = \sum_{m=1}^{\infty} \sum_{n=1}^{\infty} f_{mn} \phi_{mn}(\bar{x}, \bar{y}) \tag{28}$$

Making use of the orthogonality of eigenfuctions

$$\int_0^1 \int_0^{\sigma} \phi_{mn} \phi_{m'n'} d\bar{x}d\bar{y} = 0, \quad m \neq m', \quad \text{or} \quad n \neq n'$$

One may have ,
$$f_{mn} = \frac{\int_0^1 \int_0^{\sigma} F(\bar{x}, \bar{y}) \phi_{mn} d\bar{x}d\bar{y}}{\int_0^1 \int_0^{\sigma} \phi_{mn}^2 d\bar{x}d\bar{y}} = \frac{f_{mn}^{(1)}}{f_{mn}^{(2)}} \tag{29}$$

In which

$$\begin{aligned} f_{mn}^{(1)} &= C \int_0^1 \int_0^{\sigma} \phi_{mn} d\bar{x}d\bar{y} + \gamma \bar{E}_z \int_0^1 \int_0^{\sigma} \bar{\rho}_e \phi_{mn} d\bar{x}d\bar{y} \\ &= \frac{C [1 - \cos(\lambda_m \sigma) + \bar{\beta}_3 \lambda_m \sin(\lambda_m \sigma)] [1 - \cos(\kappa_n) + \bar{\beta}_4 \kappa_n \sin(\kappa_n)]}{\lambda_m \kappa_n} \\ &\quad + \gamma \bar{E}_z \int_0^1 \int_0^{\sigma} \bar{\rho}_e \phi_{mn} d\bar{x}d\bar{y} \end{aligned} \tag{30}$$

$$\begin{aligned} f_{mn}^{(2)} &= \int_0^1 \int_0^{\sigma} \phi_{mn}^2 d\bar{x}d\bar{y} \\ &= \left\{ \frac{\sigma}{2} (\bar{\beta}_3^2 \lambda_m^2 + 1) + \frac{\bar{\beta}_3^2 \lambda_m^2 - 1}{4 \lambda_m} \sin(2 \lambda_m \sigma) + \frac{\bar{\beta}_3}{2} [1 - \cos(2 \lambda_m \sigma)] \right\} \\ &\quad \times \left\{ \frac{\bar{\beta}_4^2 \kappa_n^2 + 1}{2} + \frac{\bar{\beta}_4^2 \kappa_n^2 - 1}{4 \kappa_n} \sin(2 \kappa_n) + \frac{\bar{\beta}_4}{2} [1 - \cos(2 \kappa_n)] \right\} \end{aligned} \tag{31}$$

Substituting (27) into equation (15), one obtains

$$\sum_{m=1}^{\infty} \sum_{n=1}^{\infty} -w_{mn} (\lambda_m^2 + \kappa_n^2) \phi_{mn} = \sum_{m=1}^{\infty} \sum_{n=1}^{\infty} f_{mn} \phi_{mn} \tag{32}$$

In which
$$w_{mn} = \frac{f_{mn}}{c_{mn}}, \quad c_{mn} = -(\lambda_m^2 + \kappa_n^2), \tag{33}$$

Based on equation (19), the dimensionless electric field in the microchannel is expressed as follows

$$\bar{E}_z = \int_0^1 \int_0^{\sigma} \bar{w} \bar{\rho}_e d\bar{x}d\bar{y} = \sum_{m=1}^{\infty} \sum_{n=1}^{\infty} w_{mn} \int_0^1 \int_0^{\sigma} \phi_{mn} \bar{\rho}_e d\bar{x}d\bar{y} \tag{34}$$

Substituting equations (30)-(33) into equation (34) yields

$$\bar{E}_z = \frac{\sum_{n=1}^{\infty} \sum_{m=1}^{\infty} \frac{C Q_{mn}}{\lambda_m \kappa_n c_{mn} f_{mn}^{(2)}} \left[1 - \cos(\lambda_m \sigma) + \bar{\beta}_3 \lambda_m \sin(\lambda_m \sigma) \right] \left[1 - \cos(\kappa_n) + \bar{\beta}_4 \kappa_n \sin(\kappa_n) \right]}{1 - \sum_{n=1}^{\infty} \sum_{m=1}^{\infty} \frac{\gamma Q_{mn}^2}{c_{mn} f_{mn}^{(2)}}} \quad (35)$$

In which

$$c_{mn} = -(\lambda_m^2 + \kappa_n^2), \quad Q_{mn} = \int_0^1 \int_0^\sigma \phi_{mn} \bar{\rho}_e d\bar{x} d\bar{y} \quad (36)$$

3. NUMERICAL FLOW SOLUTION OF MICROCHANNEL WITH WALL SLIP AND ELECTRO-VISCOUS EFFECTS

The flow equation and boundary conditions (15)-(18) can be solved by finite difference iterative method with given parameters $C, \gamma, \bar{\rho}_e, \bar{\beta}_1, \bar{\beta}_2, \bar{\beta}_3, \bar{\beta}_4$

$$\nabla^2 \bar{w} = C + \gamma \bar{\rho}_e \bar{E}_z = F(\bar{x}, \bar{y}), \quad (15)$$

where $C = \frac{\rho U a}{\mu} \frac{\partial \bar{p}}{\partial \bar{z}}$, $\gamma = \frac{\varepsilon^2 \zeta^2}{\mu \lambda_b a b}$, $\bar{\rho}_e(\bar{x}, \bar{y})$ was already solved. Uniform

square elements $\Delta \bar{x} = \Delta \bar{y}$ are used. The finite difference equation is expressed as follows

$$\frac{\bar{w}_{i+1,j} - 2\bar{w}_{i,j} + \bar{w}_{i-1,j}}{\Delta \bar{x}^2} + \frac{\bar{w}_{i,j+1} - 2\bar{w}_{i,j} + \bar{w}_{i,j-1}}{\Delta \bar{y}^2} = C + \gamma (\bar{\rho}_e)_{i,j} \bar{E}_z \quad (37)$$

The iterative scheme is written as follows

$$\bar{w}_{i,j}^n = \frac{1}{4} \left\{ \bar{w}_{i+1,j}^{n-1} + \bar{w}_{i-1,j}^{n-1} + \bar{w}_{i,j+1}^{n-1} + \bar{w}_{i,j-1}^{n-1} - \Delta \bar{x}^2 \left[C + \gamma (\bar{\rho}_e)_{i,j} \bar{E}_z^{n-1} \right] \right\} \quad (38)$$

$$\bar{E}_z^{n-1} = \int_0^1 \int_0^\sigma \bar{w}^{n-1} \bar{\rho}_e d\bar{x} d\bar{y} \quad (39)$$

The slip boundary conditions (17), (18) are imposed

$$\bar{w}_{\bar{y}=0}^n = \bar{\beta}_4 \frac{\bar{w}_{\bar{y}=\Delta \bar{y}}^{n-1} - \bar{w}_{\bar{y}=0}^{n-1}}{\Delta \bar{y}}, \quad \bar{w}_{\bar{y}=1}^n = -\bar{\beta}_2 \frac{\bar{w}_{\bar{y}=1}^{n-1} - \bar{w}_{\bar{y}=1-\Delta \bar{y}}^{n-1}}{\Delta \bar{y}}, \quad (40)$$

$$\bar{w}_{\bar{x}=0}^n = \bar{\beta}_3 \frac{\bar{w}_{\bar{x}=\Delta\bar{x}}^{n-1} - \bar{w}_{\bar{x}=0}^{n-1}}{\Delta\bar{x}}, \quad \bar{w}_{\bar{x}=\sigma}^n = -\bar{\beta}_1 \frac{\bar{w}_{\bar{x}=\sigma}^{n-1} - \bar{w}_{\bar{x}=\sigma-\Delta\bar{x}}^{n-1}}{\Delta\bar{x}}, \quad (41)$$

Where the superscripts $n, n-1$ denote the iterative times. $\bar{w}_{i,j}^0 = 0$ are taken as initial solutions. The initial electric field are calculated $\bar{E}_z^0 = \int_0^1 \int_0^\sigma \bar{w}^0 \bar{\rho}_e d\bar{x}d\bar{y}$. Repeat iterative calculations until convergent solutions are obtained.

4 STUDY EXAMPLES AND DISCUSSION

The typical data of electrokinetic flows in rectangular microchannel are specified: Example 1 : square section $\sigma = b/a = 1$, characteristics velocity $U = 0.01 m/s$, DEL parameter $\sigma_2 = -1.95$, electrokinetic length $\kappa a = 20$, slip lengths $\bar{\beta}_1 = \bar{\beta}_2 = \bar{\beta}_3 = 0.06$, wall Zeta potentials $\bar{\zeta}_1 = \bar{\zeta}_2 = \bar{\zeta}_3 = 0.5$ on PDMS walls, $\bar{\beta}_4 = 0$, $\bar{\zeta}_4 = 1.0$ on glass wall, pressure gradient parameter $C = -13.6$, $m = n = 30$ for calculating of the analytic solutions. 200×200 uniform square grids are used for the numerical solutions. The flow velocity profile of channel section is shown in figure (2), where $\gamma = 0.0004$.

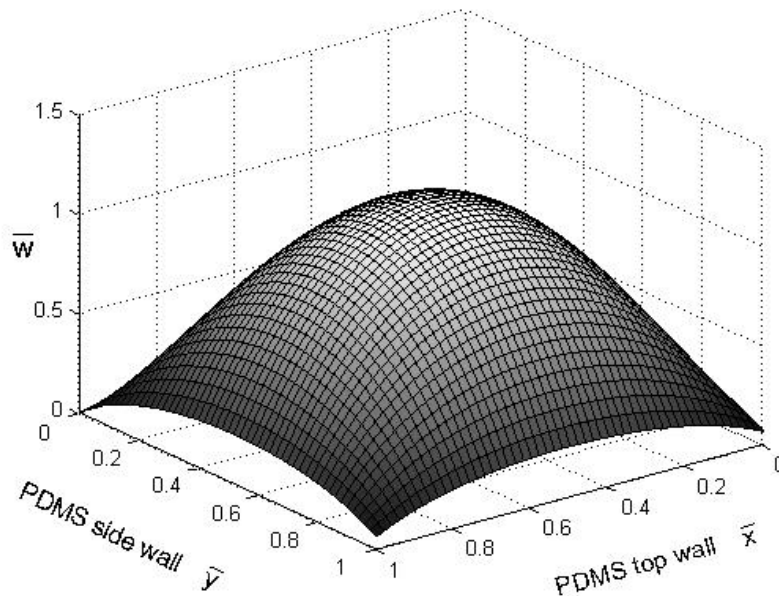


Fig. 2 Velocity profile on rectangular channel section with wall slip and electro-viscous effects $b/a = 1$

Wall slip velocities can be seen on PDMS top wall and side walls. The flow velocity profile on PDMS top wall of channel is shown in figure (3). The analytic solutions well agree with the numerical solutions. The wall slip velocity is about 25% of the maximum velocity of channel in present example. The slip velocity at wall corners are much smaller then that at the wall center. The flow velocity profile on PDMS side wall of channel is shown in figure (4) where no slip velocity on glass bottom wall ($y=0$) is found. The flow velocity profile along horizontal central line ($y=0.5$) of channel section is shown in figure (5), and the flow velocity profile along vertical central line ($x=0.5$) of channel section is shown in figure (6). Due to PDMS wall slip it can be seen that, in present example, the maximum flow velocity of the channel is about 118% of the maximum velocity in cases without electro-viscous effect ($\gamma = 0$). It is also found that the electro-viscous effect decreases flow velocities and flow rate of the channel in all cases.

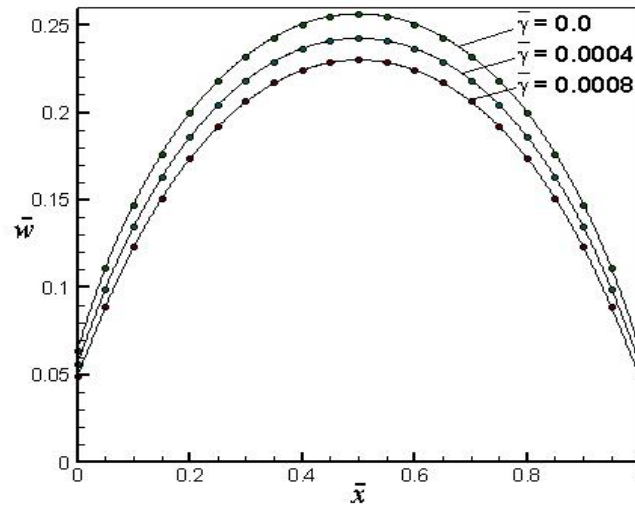


Fig. 3 Slip velocity profile on PDMS top wall ($y=1$), $b/a=1$

— Analytic solutions, • • • Numerical solutions

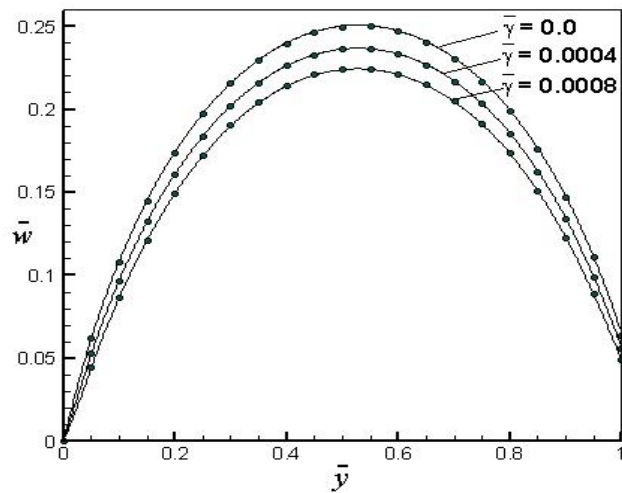


Fig. 4 Slip velocity profile on PDMS side wall ($x=0$), $b/a = 1$

— Analytic solutions, • • • Numerical solutions

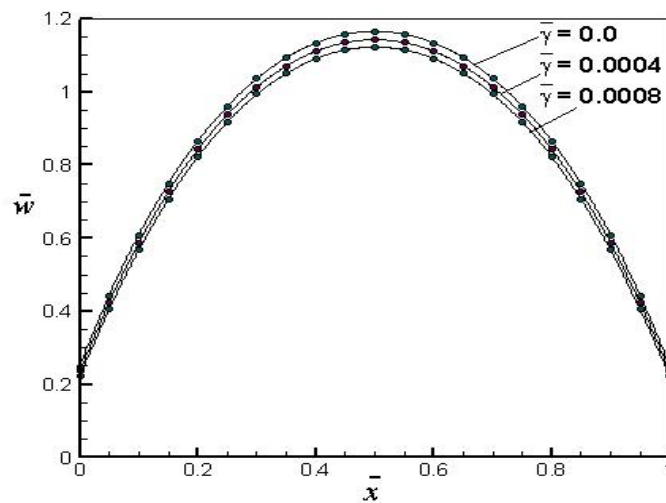


Fig. 5 Velocity profile along horizontal central line ($y=0.5$) of the channel section, $b/a = 1$

— Analytic solutions, • • • Numerical solutions

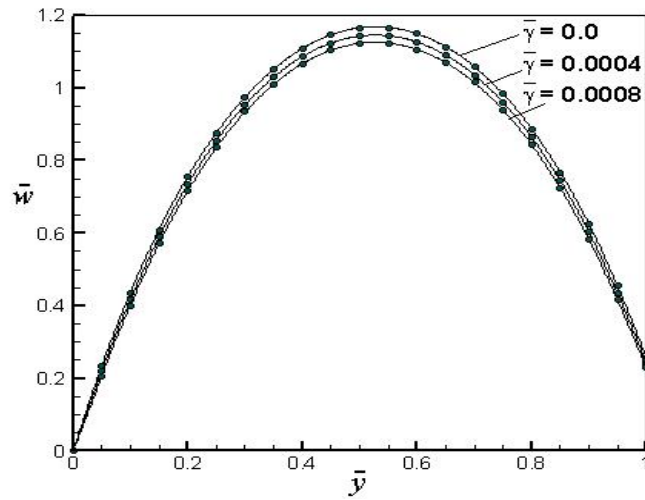


Fig. 6 Velocity profile along vertical symmetrical line ($x=0.5$) of the channel section, $b/a=1$

— Analytic solutions, • • • Numerical solutions

The relationship of the maximum flow velocity of the channel and PDMS wall slip lengths is shown in figure (7). The maximum flow velocity increases with increase of the wall slip lengths, and decreases with increase of electro-viscous number. Similar behaviors are found for channel flow rate and flow-induced electric fields, as shown in figures (8), (9), respectively. It indicates that the wall slippage enhances the electro-viscous effects on flows when pressure gradient is fixed.

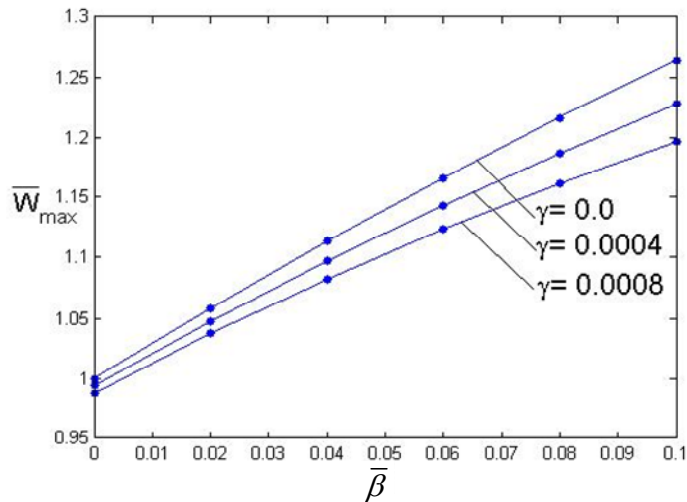


Fig. 7 The maximum flow velocity versus PDMS wall slip lengths, $b/a=1$

— Analytic solutions, • • • Numerical solutions

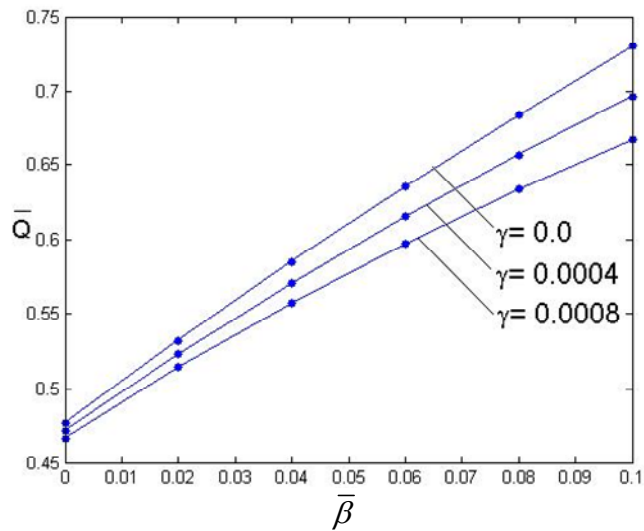


Fig. 8 The flow rate of the channel versus PDMS wall slip lengths, $b/a = 1$

— Analytic solutions, • • • Numerical solutions

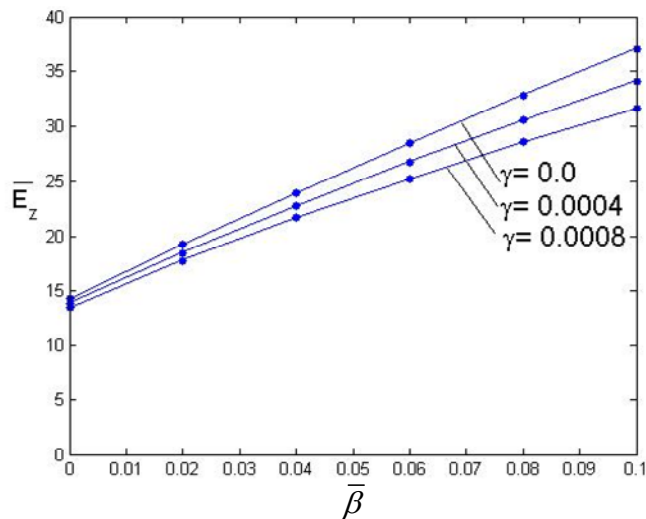


Fig. 9 The flow-induced electric field versus PDMS wall slip lengths, $b/a = 1$

— Analytic solutions, • • • Numerical solutions

Example 2 : narrow section $\sigma = b/a = 5$, 1000×200 uniform square grids are used for the numerical solutions. The rest of parameters are the same as the example 1. The flow velocity profile of channel section is shown in figure (10) in which $\gamma = 0.0004$.

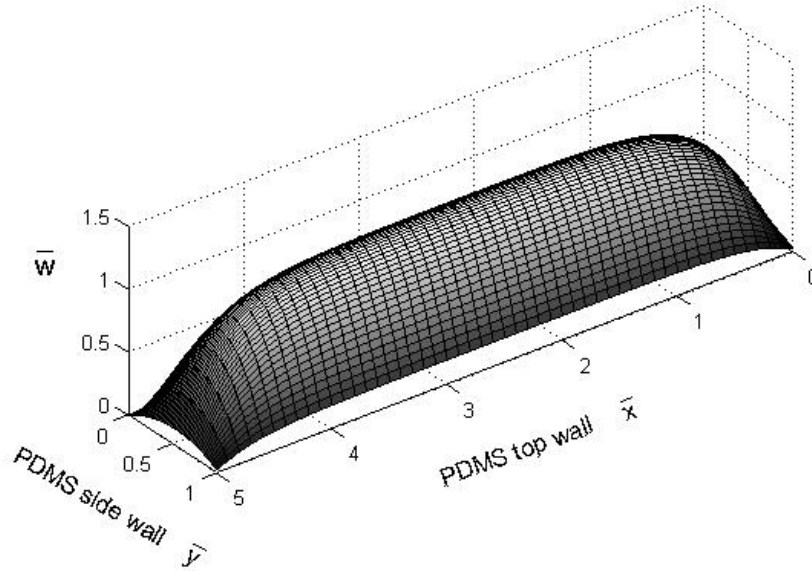


Figure 10 The velocity profile on rectangular channel section with wall slip and electro-viscous effects when $b/a = 5$

It can be seen that the velocity profile of section is flat and uniform in direction of wide wall in middle part of the channel section. The slip velocity profile on PDMS top wall (wide wall) and side wall (narrow wall) are shown in figures (11), (12), respectively.

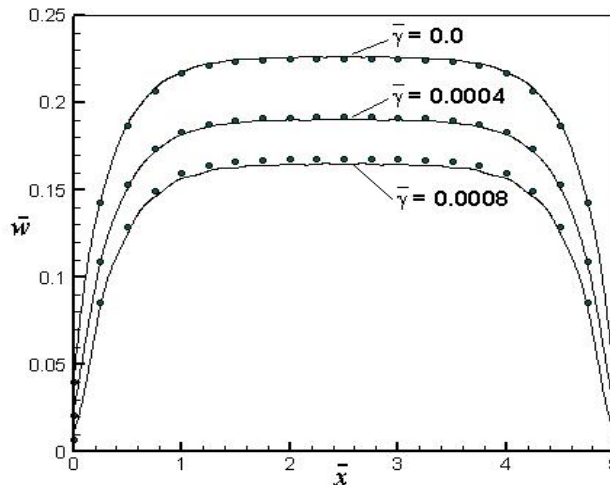


Figure 11 The slip velocity profile on PDMS top wall ($y=1$) when $b/a = 5$

— Analytic solutions, • • • Numerical solutions

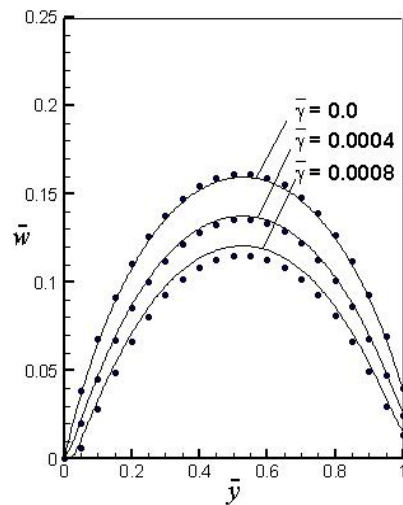


Figure 12 The slip velocity profile on PDMS side wall ($x=0$), $b/a = 5$
 ——— Analytic solutions, • • • Numerical solutions

The slip velocities on PDMS top wall tend to be uniform, and larger in magnitude than that on PDMS side wall where the slip velocity shows parabolic profile. The slip velocities at section corners are much smaller than that of wall center. It is also found that the behavior of maximum velocity, channel flow rate and flow-induced electric field are similar to those in cases of square section ($b/a = 1$) discussed above, as shown in figures (13), (14), (15), respectively. The PDMS wall slippage increases flow velocities, flow rate and flow-induced electric field, the electro-viscous effect decreases flow velocity and channel flow rate in all cases.

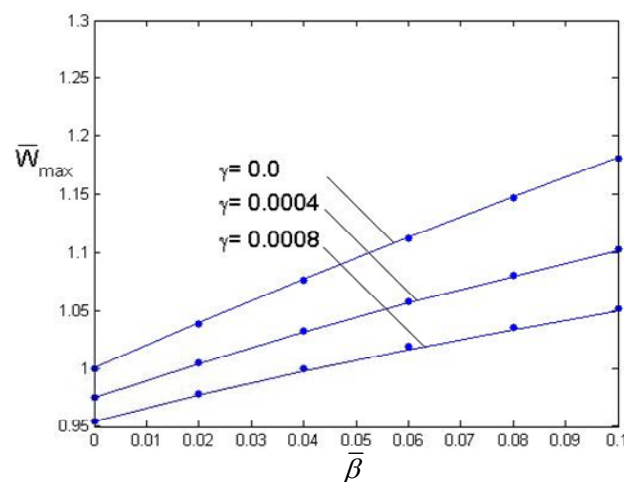


Fig. 13 The maximum flow velocity versus PDMS wall slip lengths, $b/a = 5$

———— Analytic solutions, • • • Numerical solutions

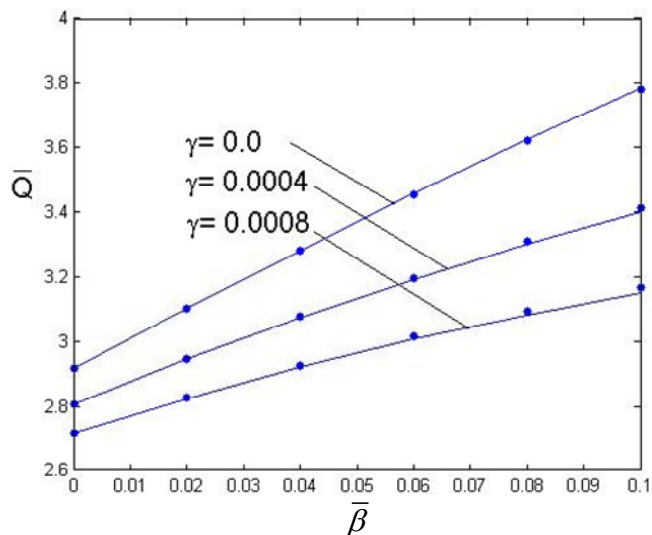


Fig. 14 The channel flow rate versus PDMS wall slip lengths, $b/a = 5$

— Analytic solutions, • • • Numerical solutions

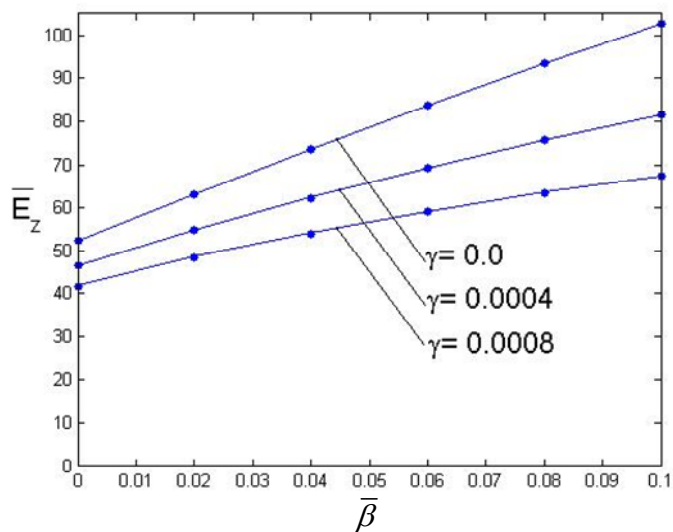


Fig. 15 The flow-induced electric field versus PDMS wall slip lengths, $b/a = 5$

— Analytic solutions, • • • Numerical solutions

5 CONCLUSION REMARK

The pressure-driven flow in uniform rectangular microchannel made of PDMS/

GLASS was studied in this work. The effects of the wall slip and the electro-viscosity on flows were investigated. An analytic solution of flow velocity and flow-induced electric field was presented and in good agreement with numerical solutions. The slip velocity of PDMS wall increases flow velocities and flow rate of microchannel, the electro-viscous effect of electric double layer decreases flow velocity and flow rate of microchannel. PDMS wall slip velocity amplifies flow-induced electric field and enhances electro-viscous effect on flows in microchannel. For a microchannel with narrow section the slip flow velocity on wide wall tends to be uniform, and \bar{v}_x and \bar{v}_y are larger than those on the narrow wall.

ACKNOWLEDGMENTS. This work is supported by Natural Science Foundation of China (Grant No.10872076)

Appendix A

The dimensionless Poisson-Boltzmann equation of electric double layer reads as follows

$$\nabla^2 \bar{\varphi} = \alpha_1 \sinh(\alpha_2 \bar{\varphi}), \quad \bar{\rho}_e = \nabla^2 \bar{\varphi} \quad (13)$$

where $\alpha_2 = ze\zeta/(K_b T)$, $\alpha_1 = (\kappa a)^2/\alpha_2$. Finite difference scheme with uniform square grids ($\Delta \bar{x} = \Delta \bar{y}$) is used to solve P-B equation (13) in rectangular channel section. The finite difference scheme is written as follows

$$\frac{\bar{\varphi}_{i+1,j} - 2\bar{\varphi}_{i,j} + \bar{\varphi}_{i-1,j}}{\Delta \bar{x}^2} + \frac{\bar{\varphi}_{i,j+1} - 2\bar{\varphi}_{i,j} + \bar{\varphi}_{i,j-1}}{\Delta \bar{y}^2} = \alpha_1 \sinh(\alpha_2 \bar{\varphi}_{i,j}) \quad (A-2)$$

Iterative algorithm of equation (A-2) is expressed as

$$\bar{\varphi}_{i,j}^n = \frac{\bar{\varphi}_{i+1,j}^{n-1} + \bar{\varphi}_{i-1,j}^{n-1} + \bar{\varphi}_{i,j+1}^{n-1} + \bar{\varphi}_{i,j-1}^{n-1} - \Delta \bar{x}^2 \alpha_1 \sinh(\alpha_2 \bar{\varphi}_{i,j}^{n-1})}{4} \quad (A-3)$$

The boundary conditions (14) are imposed

$$\begin{aligned} \bar{\varphi} &= \bar{\zeta}_3, & \bar{x} &= 0; & \bar{\varphi} &= \bar{\zeta}_1, & \bar{x} &= \sigma, \\ \bar{\varphi} &= \bar{\zeta}_4, & \bar{y} &= 0, & \bar{\varphi} &= \bar{\zeta}_2, & \bar{y} &= 1, \end{aligned} \quad (14)$$

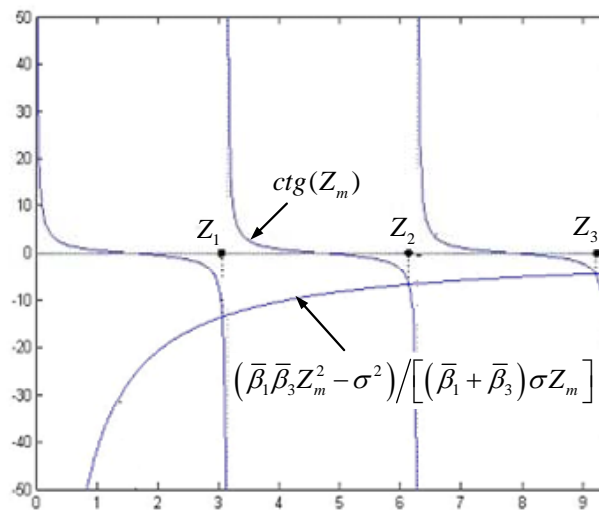
Where superscripts n , $n-1$ are the iterative times, $\bar{\varphi}_{i,j} = 0$ are taken as initial values. When convergent solutions are obtained the charge density can be calculated from $\bar{\rho}_e = \alpha_1 \sinh(\alpha_2 \bar{\varphi})$.

Appendix B

The eigenvalue equation (25) $ctg(\lambda_m \sigma) = \frac{\overline{\beta_1 \beta_3} \lambda_m^2 - 1}{(\overline{\beta_1 + \beta_3}) \lambda_m}$ can be rewritten as

$$ctg(Z_m) = \frac{\overline{\beta_1 \beta_3} Z_m^2 - \sigma^2}{(\overline{\beta_1 + \beta_3}) \sigma Z_m}, \quad Z_m = \sigma \lambda_m, \quad \text{as shown in following figure.}$$

Eigenvalues Z_m can be solved by Newtonian iterative algorithm.



REFERENCES

- [1] Christian Davidson, Xiangchun Xuan , Electrokinetic energy conversion in slip nanochannels , Journal of Power Sources, 179 (2008), 297–300.
- [2] Derek C. Tretheway and Carl D. Meinhart, Apparent fluid slip at hydrophobic microchannel walls, Physics of Fluids, 14 (3), (2002), L9-L12.
- [3] Derek C. Tretheway and Carl D. Meinhart, A generating mechanism for apparent fluid slip in hydrophobic microchannels, Physics Fluids, 16 (5) , (2004), 1509-1515.

- [4] J. Baudry, E. Charlaix , A. Tonck and D. Mazuyer, Experimental evidence for a large slip effect at a non-wetting fluid-solid interface, *Langmuir*, 17 (2001), 5232-5236.
- [5] Jean-Louis Barrat, Large slip effect at a non-wetting fluid-solid interface, *Physical Review Letters*, 82 (1999), 4671-4674.
- [6] Jia Ou, Blair Perot, and Jonathan P. Rothstein, Laminar drag reduction in microchannels using ultrahydrophobic Surfaces, *Physics of Fluids*, 16 (12), (2004), 4635-4643.
- [7] Myung-Suk Chun, Tae Seok Lee and Kangtaek Lee, Microflow of dilute colloidal suspension in narrow channel of microfluidic-chip under Newtonian fluid slip condition, *Korea-Australia Rheology Journal*, 17 (4), (2005), 207-215.
- [8] Pierre Joseph, Patrick Tabeling, Direct measurement of the apparent slip length, *Physics Review*, E 71 (2005) , 035303(R).
- [9] R.Pit, H. Hervet and L. Léger, Direct experimental evidence of slip in hexadecane: solid interfaces, *Physical Review Letters*, 85 (5), (2000), 980-983.
- [10] Remmelt Pit, Hubert Hervet and Liliane L'éger, Friction and slip of a simple liquid at a solid surface , *Tribology Letters*, 7 (1999), 147–152.
- [11] Yingxi Zhu and Steve Granick, Limits of the hydrodynamic no-slip boundary condition , *Physical Review Letters*, 88(11), (2002), 106102.
- [12] Edouard Brunet¹ and Armand Ajdari, Generalized Onsager relations for electrokinetic effects in anisotropic and heterogeneous geometries, *Physical Review*, E 69 (2004), 016306.
- [13] Yongqiang Ren and Derek Stein, Slip-enhanced electrokinetic energy conversion in nanofluidic channels, *Nanotechnology*, 19 (2008), 195707.
- [14] Chun Yang, Dongqing Li, Jacob H. Masliyah, Modeling forced liquid convection in rectangular microchannels with electrokinetic effects, *Int. J. Heat Mass Transfer*, 41 (1998), 4229-4249.
- [15] Dongqing Li, *Electrokinetics in Microfluidics*, Elsevier academic press, 2004.

- [16] J. Lyklema, Fundamentals of interface and colloidal science, Academic Press, New York, Vol. II, 1995.
- [17] Liqing. Ren , Weilin Qu, Dongqing Li, Interfacial electrokinetic effects on liquid flow in microchannels, Int .J. Heat Mass Transfer, 44 (2001) , 3125-3134.
- [18] Myung-Suk Chun, Sang-Yang Lee, Seung-Man Yang, Estimation of Zeta-potential by electrokinetic analysis of ionic fluid flows through a divergent microchannel, J. Colloid and Interface Sci., 266(2003), 120-126.
- [19] R. J. Hunter, Zeta potential in colloidal science, Principle and Application, Academic Press, New York, 1981.

Received: February, 2009